Al2O3 preforms infiltrated with poly(methyl methacrylate) for dental prosthesis manufacturing

applied sciences

MDPI

Article

Al_2O_3 Preforms Infiltrated with Poly(methyl methacrylate) for Dental Prosthesis Manufacturing

Olimpia Crispim da Silveira [1], Alisson Mendes Rodrigues [2], Maziar Montazerian [2], Hélio de Lucena Lira [2,*], Francesco Baino [3,*] and Romualdo Rodrigues Menezes [2]

[1] Programa de Pós-Graduação em Ciência e Engenharia de Materiais (PPG-CEMat), Universidade Federal de Campina Grande, Av. Aprígio Veloso-882, Bodocongó, Campina Grande 58429900, PB, Brazil; olimpiacsilveira1803@gmail.com

[2] Unidade Acadêmica de Engenharia de Materiais, Centro de Ciências e Tecnologia, Universidade Federal de Campina Grande, Av. Aprígio Veloso-882, Bodocongó, Campina Grande 58429900, PB, Brazil; alisson.mendes@professor.ufcg.edu.br (A.M.R.); maziar_montaz@yahoo.com (M.M.); romualdo.menezes@ufcg.edu.br (R.R.M.)

[3] Institute of Materials Physics and Engineering, Department of Applied Science and Technology (DISAT), Politecnico di Torino, Corso Duca degli Abruzzi 24, 10129 Torino, Italy

* Correspondence: helio.lira@ufcg.edu.br (H.d.L.L.); francesco.baino@polito.it (F.B.)

Abstract: The combination of biocompatible polymers and ceramics shows great promise in the development of composites with suitable mechanical properties for dental applications. In an attempt to further expand this research line, Al_2O_3 commercial powders (Vitro-ceram, Alglass, In-ceram) were sintered at 1400 °C for 2 h and infiltrated with poly(methyl methacrylate) for potential use in dental prostheses. The infiltration was performed using a homemade apparatus under a pressure of 7 bar for 6 and 12 h. The microstructure (studied using a scanning electron microscope), Archimedes density, 3-point bending flexural strength and Vickers hardness of the prepared composites were assessed and quantitatively compared. In general, microstructural analyses showed ceramic- and polymer-based interpenetrating network in all materials. The preforms infiltrated for 12 h showed superior properties; among them, the Vitro-ceram-based composite also demonstrated a near-zero open porosity and optimum mechanical characteristics. Specifically, its density, strength and hardness were 2.6 ± 0.07 g/cm^3, 119.3 ± 5.0 MPa and 1055.1 ± 111.0 HV, respectively, passing the acceptance criteria of ISO 6872 and making it suitable for consideration as a metal-free structure for dental crowns and fixed partial prostheses until three anterior units.

Keywords: composite; PMMA; alumina; dental prosthesis; infiltration; mechanical properties

Citation: Crispim da Silveira, O.; Rodrigues, A.M.; Montazerian, M.; de Lucena Lira, H.; Baino, F.; Menezes, R.R. Al_2O_3 Preforms Infiltrated with Poly(methyl methacrylate) for Dental Prosthesis Manufacturing. *Appl. Sci.* **2021**, *11*, 7583. https://doi.org/10.3390/app11167583

Academic Editor: Giovanni Bruno

Received: 5 July 2021
Accepted: 16 August 2021
Published: 18 August 2021

1. Introduction

The global market for dental materials is surpassing 10 billion dollars [1]. The main driving forces for this growth are improving the dentists' workflow and increasing patients' comfort. Therefore, remarkable investigations have been conducted to develop improved or new restorative dental materials with enhanced properties. Among these materials, resin-based composites, ceramics, glass-ceramics or polymer-infiltrated ceramics are of great importance. The microstructural characterization and determination of the mechanical properties of these materials are the first steps to understand their behavior in restorative dentistry [2,3].

The resin-based composites such as glass ionomer cements and whisker-reinforced resins are among the main dental restorative materials. These composites are composed of a polymeric matrix and reinforcing inorganic fillers. The type, morphology, content and structure of the fillers and interface directly dictate the mechanical and aesthetic properties of the composites. The development of new fillers such as nano-whiskers and nanoparticles has resulted in considerable improvements of the composite properties [4,5].

The key criteria for selecting a filler include the biocompatibility, mechanical and optical characteristics. Additionally, the dimensional changes, final density, fracture toughness and machinability resulting from the polymerization are determined by the polymer matrix, which commonly includes bisphenol A-glycidyl methacrylate (Bis-GMA), urethane dimethacrylate (UDMA), urethane trimethacrylate (UTMA) and ethoxylated bisphenol A-glycol dimethacrylate (Bis-EMA) [4,5].

Nevertheless, the clinical performance of resin-based composites is still inferior to the performance of ceramic or glass-ceramic restorations considering the marginal adaptation, color match, anatomic form and mechanical strength [6]. A three-year clinical study revealed that these restorations have inferior aesthetic and wear resistance compared to all-ceramic restorations [7]. However, the use of ceramics/glass-ceramics in many applications suffers from their low fracture toughness and high susceptibility to slow crack growth [8]. The combined properties of these two groups of materials, such as Al_2O_3 ceramics and resin-based composites, could be a solution for overcoming the shortcomings of restorative materials. For example, combining Young's modulus of resin-based composites, which is similar to the dentin Young's modulus, with the long-lasting strength, hardness and aesthetics of ceramics, would be ideal for a restorative material. The polymer-infiltrated ceramic (PIC) network may offer an alternative solution. The fabrication process of this type of material requires the following two steps: first, a porous pre-sintered ceramic network is produced and then, this network is infiltrated with a polymer by capillary action. The flexural strength, elastic modulus, hardness and strain at failure of PIC structures have been reported in previous studies [9,10], showing similar properties to the tooth structure, which encourages further studies on these materials. PMMA is commonly used for prosthetic dental applications, including the fabrication of artificial teeth, denture bases, dentures, obturators, orthodontic retainers, temporary or provisional crowns and the repair of dental prostheses. Other applications of PMMA in dentistry include occlusal splints, printed or milled casts, dies for treatment planning and the embedding of tooth specimens for research purposes. The distinctive properties of PMMA, such as its low density, aesthetics, cost-effectiveness, ease of handling and tailorable physical and mechanical properties, make it a suitable and popular biomaterial for these applications. Several chemical modifications and mechanical reinforcement techniques using various types of fibers, nanoparticles and nanotubes have been reported to improve the properties (thermal behavior, water sorption, solubility, impact strength, flexural strength) of PMMA [10]. For example, the addition of Al_2O_3 nanoparticles to PMMA resulted in better biocompatibility [11]. The addition of silane-treated alumina particles remarkably improved the mechanical properties—mainly the compressive and flexural strengths and wear resistance [12]. Al_2O_3 has no significant effects on the water sorption or surface roughness of PMMA [13] but significantly improves the thermal conductivity of the polymer [14]. The present study aims to determine some key mechanical properties of the newly synthesized porous networks of the Al_2O_3 commercial powder infiltrated with poly(methyl methacrylate) (PMMA), testing the hypothesis that the new material has properties ranging between Al_2O_3 and resin-based composites [10]. To the best of our knowledge, the development and characterization of PMMA-infiltrated Al_2O_3 for dental applications has not been reported before. Our objective was to develop a relatively cheap, sizeable restorative prosthesis that new technologies such as CAD/CAM could adapt.

2. Materials and Methods

2.1. Raw Materials

In this research, the following three Al_2O_3 commercial powders were used: Vitro-ceram supplied by Angelus (Londrina, PR, Brazil), Alglass supplied by Celmat (São Paulo, SP, Brazil) and In-ceram supplied by Vita Zahnfabrik (Berlin, Germany), see Figure 1. The other raw materials used were methyl methacrylate monomer (Neon, São Paulo, SP, Brazil) and benzoyl peroxide (Vetec, São Paulo, SP, Brazil).

Figure 1. Al_2O_3 commercial powders used in this research (Vitro-ceram, Alglass and In-ceram).

2.2. Preparation of the Al_2O_3 Preforms

Samples with dimensions of 30 × 5 × 4 mm^3 were prepared for each type. For this, 2 g of Al_2O_3 commercial powders were uniaxially pressed (66 MPa for 30 s) and sintered in an electric oven. The samples preparation was accomplished according to ISO 6872 standard [15]. The sintering protocol involved heating the samples from room temperature to 1400 °C at a rate of 5 °C/min, holding the samples at this temperature for 2 h and cooling them down inside an electric oven (average cooling rate ~5 °C/min).

2.3. Methyl Methacrylate Monomer-Infiltration

The methyl methacrylate monomer-infiltration into the Al_2O_3 preforms was accomplished with the aid of a homemade system. It was composed of a stainless steel vacuum chamber (diameter = 170 mm, height = 230 mm and thickness = 6 mm), iron magnet (150 mm × 60 mm × 15 mm; mass = 60 g), a lid of the stainless steel vacuum chamber having a place for one iron magnet, a borosilicate beaker and a pressure system, see Figure 2a–b. The infiltration procedure was divided into three steps. In the first step, the samples were fixed in the chamber slid with an iron magnet. The vacuum chamber was then sealed using an o-ring fixed to a metal structure on a triangular tripod with an adjustable spindle. For the second step, firstly the system was kept under vacuum (750 mmHg) for 30 min. Such a procedure was accomplished to eliminate gases present in the samples. The iron magnet was removed in the third step, and the samples were dropped into a beaker containing methyl methacrylate monomer and benzoyl peroxide initiator in 1:1 (vol/vol) proportion. The Al_2O_3 preforms were kept in the beaker for 6 and 12 h under pressure equal to 7 bar. In the last step, the monomer-infiltrated Al_2O_3 samples were put in a hermetically sealed glass bottle and polymerization occurred in an oven at 60 °C. Table 1 summarizes the name of the Al_2O_3 preforms prepared with their respective infiltration times and estimated amount of PMMA (vol.%) infiltration.

Table 1. Summary of conditions for preparation of samples, infiltration time and the estimated amount of PMMA (vol.%) infiltration.

Suppliers	Specimens Conditions	Time (h)	Estimated Amount of PMMA (vol.%)
Alglass	Without infiltration	0	0
In-ceram	Without infiltration	0	0
Vitro-ceram	Without infiltration	0	0
Alglass	With infiltration	6	13
In-ceram	With infiltration	6	12
Vitro-ceram	With infiltration	6	9
Alglass	With infiltration	12	16
In-ceram	With infiltration	12	20
Vitro-ceram	With infiltration	12	>9

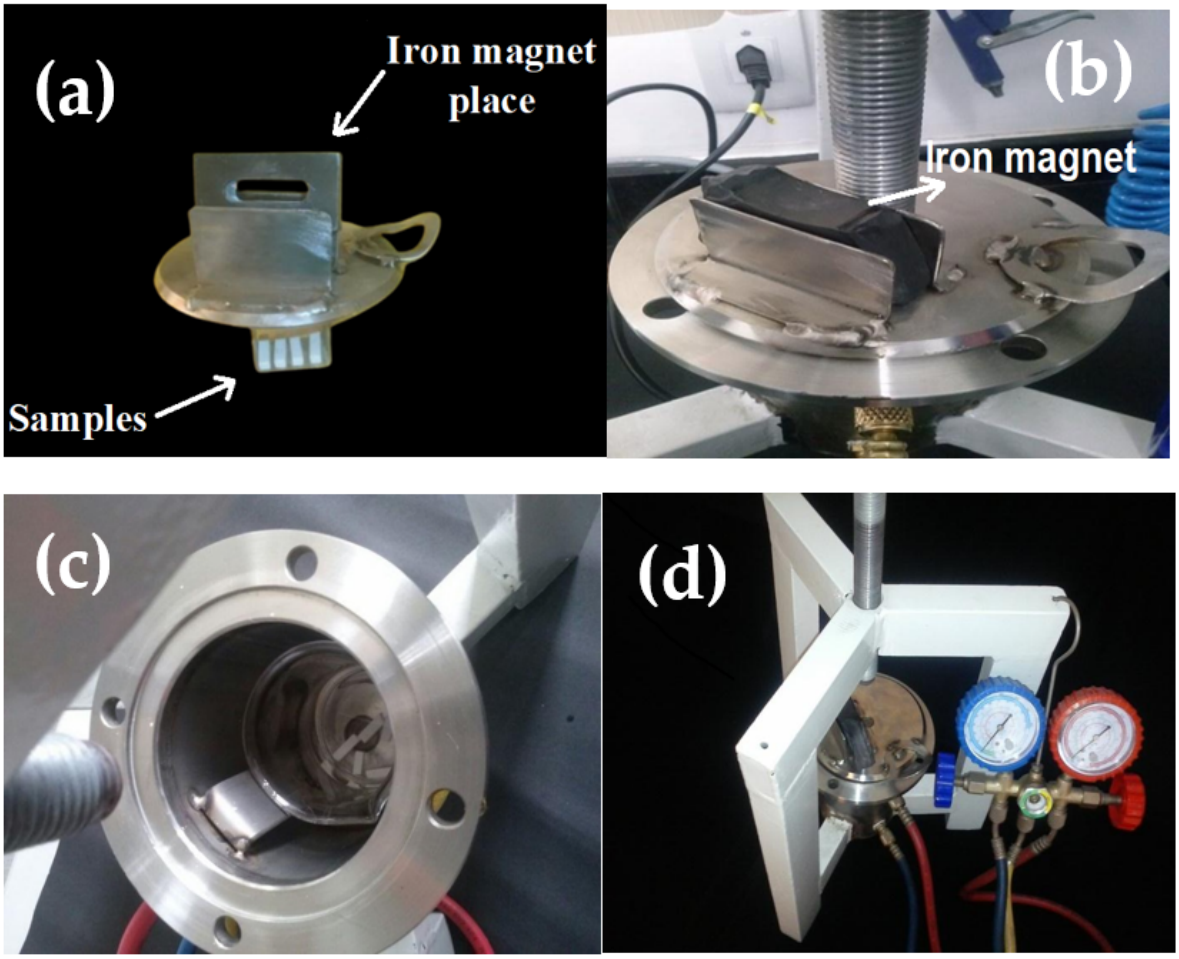

Figure 2. Configuration of the homemade system designed for infiltration of PMMA into the sintered Al_2O_3 commercial samples. (**a**) A lid of the stainless steel for vacuum chamber above which one iron magnet is placed, (**b**) iron magnet (150 mm × 60 mm × 15 mm; mass = 60 g) put over the lid, (**c**) a stainless steel vacuum chamber (diameter = 170 mm, height = 230 mm and thickness = 6 mm) inside which a beaker and samples are shown, and (**d**) the whole configuration of infiltration system connected to vacuum pressure adjustment.

2.4. Characterizations and Physico-Mechanical Properties

The chemical composition of all Al_2O_3 commercial powders was determined using Energy-Dispersive X-ray Spectroscopy (EDX) (SHIMADZU, EDX 720, Kyoto, Japan). The qualitative phase analysis was accomplished by X-ray diffraction (XRD) using a Bruker-D2Phaser diffractometer (CuKα, 40 kV/30 mA). All XRD analyses were carried out at room temperature, with a goniometer speed of 2°/min, an angular step of 0.02° and a counting time of 0.6 s. The diffraction peaks observed were indexed using the Search Match® Program and the JCPDS database. The particle size distribution was measured by wet granulometric analysis (in deflocculated dispersion) using a laser diffraction equipment (Cilas, 1064 LD).

After infiltration, sample surface and cross-section were characterized by a scanning electron microscope (SEM) using SSX-550 Shimadzu (Kyoto, Japan). Vickers' microhardness was estimated using an HMV-G21D Tester from Shimadzu (Kyoto, Japan). Ten samples were used for each composition. The indentation load and time were 9.8 N and 15 s, respectively, which is recommended by ASTM C 1327-08. According to the ISO 6872:2015 standard, a universal testing machine of Instron model 5582 was employed to determine the three-point bending strength. Such testing was performed on 10 samples for each composition (sized to 30 × 5 × 4 mm^3). The distance between the supports and test speed were 25 mm and 0.5 mm/min, respectively.

The Archimedes method was used to measure water absorption, apparent porosity and bulk density. Before immersion in distilled water, sintered samples were dried at 60 °C for 24 h to calculate their dry weight. Then, the samples were immersed in distilled water for 24 h to obtain the wet weight and the immersed weight. All samples were weighed on a Shimadzu balance, model AY 220.

The *t*-test and Tukey media comparison, using a significance level of 5%, was used for statistical analysis of measured values.

3. Results and Discussion

3.1. Crystalline Phases, Chemical Analysis and Particle Size Distributions of the Al_2O_3 Commercial Powders

The XRD patterns (Figure 3a–c) and EDX-chemical analysis (Table 2) obtained for Alglass, Vitro-ceram and In-ceram samples show that the α-alumina (JCPDS standard 10-0173) is the prominent crystalline constituent. Low-intensity ZrO_2 peaks were also identified on the XRD pattern of the Vitro-ceram samples (Figure 3c). In accordance with the XRD results, the chemical analysis indicated a discrete amount of zirconia (0.30 wt.%) in the Vitro-ceram. A minor amount of SiO_2 (0.2 wt.%) and P_2O_5 (0.2 wt.%) in the Alglass and Vitro-ceram samples, respectively, were also identified.

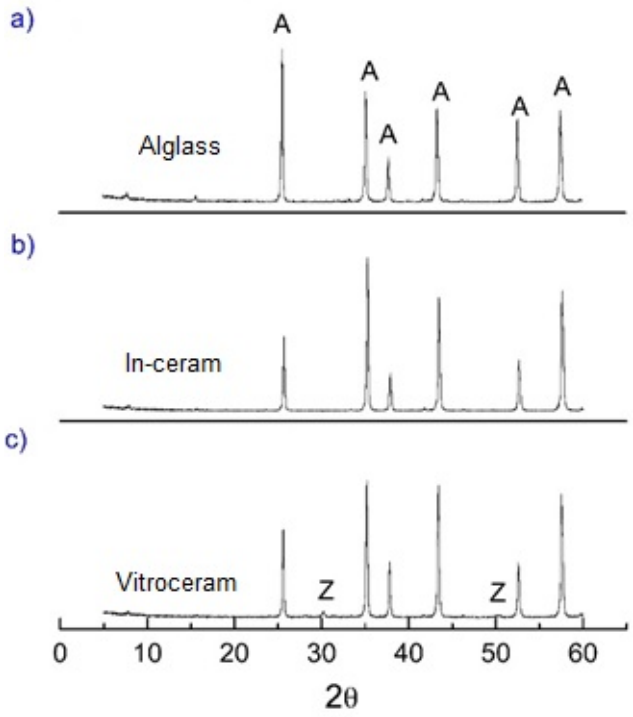

Figure 3. X-ray diffraction spectra of alumina samples: (**a**) Alglass, (**b**) In-ceram and (**c**) Vitro-ceram. A and Z denote α-alumina and zirconia phases, respectively.

Table 2. EDX chemical analysis obtained for Alglass, Vitro-ceram and In-ceram.

Samples	(wt.%)				
	Al_2O_3	SiO_2	P_2O_5	ZrO_2	Other Oxides
Alglass	99.6	0.2	–	–	0.02
In-ceram	99.8	–	–	–	0.02
Vitro-ceram	98.9	–	0.5	0.3	0.30

Figure 4 shows the particle size distribution of Alglass, Vitro-ceram and In-ceram powders. The Alglass presented a heterogeneous and trimodal particle size distribution,

in which the maximum sizes measured were 0.5, 11.5 and 50 µm. This type of particle distribution contributes to excellent compaction in the pressing and sintering process. The In-ceram presented a monomodal particle size distribution ranging from 0.1 µm to around 30 µm, where the most significant percentage of particles falls close to 16 µm. The Vitro-ceram powder also showed a bimodal distribution of particles with a maximum between 0.3 and 5.0 µm; this sample exhibited the smallest particle size distribution. The mixture of particles with different diameters observed can favor higher compaction, with smaller particles occupying the empty spaces that lie between the larger particles. The systems with a wide range of particle diameters will densify better [16].

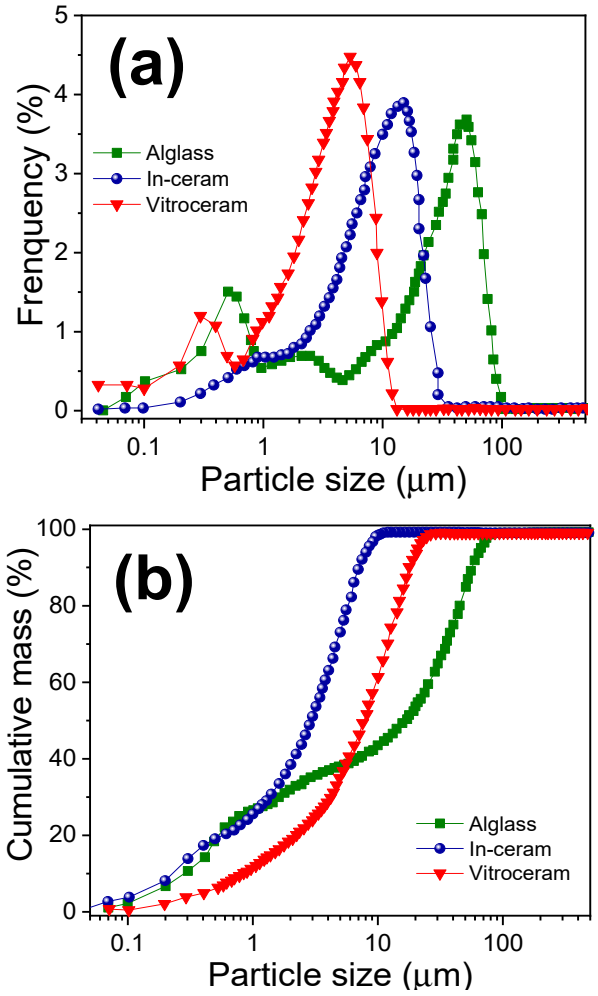

Figure 4. (**a**) Distribution and (**b**) cumulative mass of particle size of Alglass, In-ceram and Vitro-ceram powders.

3.2. SEM Investigation and Physico-Mechanical Properties of the Poly(methyl methacrylate)-Infiltrated Al_2O_3 Samples

Figure 5 shows the Alglass, Vitro-ceram and In-ceram samples before poly(methyl methacrylate) infiltration and sintering at 1400 °C for 2 h. The color difference among the samples might be due to the impurities contained in the starting powders. Vitro-ceram with a small amount of ZrO_2 was the whitest.

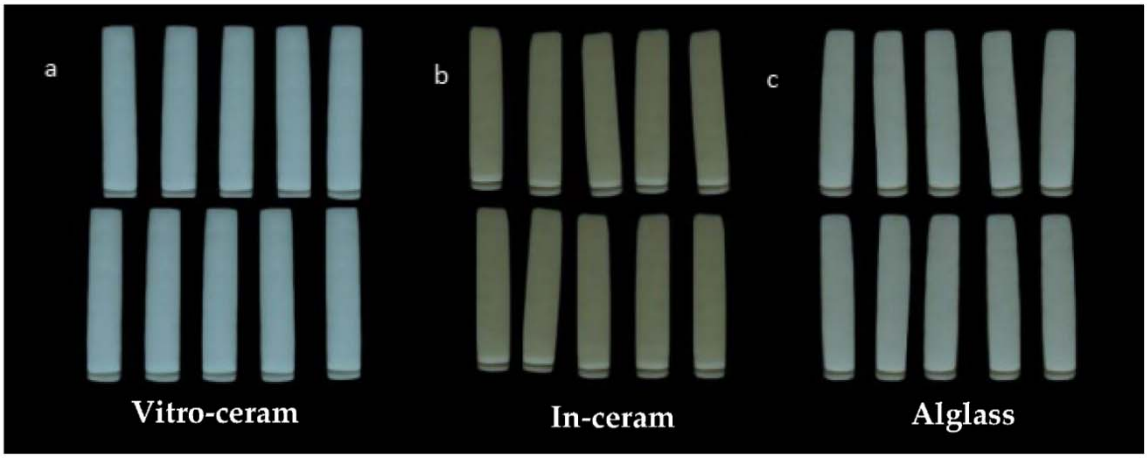

Figure 5. (**a**) Alglass, (**b**) Vitro-ceram and (**c**) In-ceram samples before infiltration and sintered at 1400 °C for 2 h.

As an example, Figure 6a–b show the SEM images acquired from the Vitro-ceram sample cross-section, which was infiltrated with PMMA for 6 h. It seems that the PMMA infiltration is efficient and considerably fills the porosities, but there are some heterogeneous pores still visible at a higher magnification (Figure 6c). Figure 6d shows an SEM image acquired from the cross-section of the sample, which proves enough infiltration of PMMA after 12 h. The depth of infiltrated polymer varies from 173 to 180 µm, forming a rigid, defect-free surface that could potentially inhibit crack initiation and propagation.

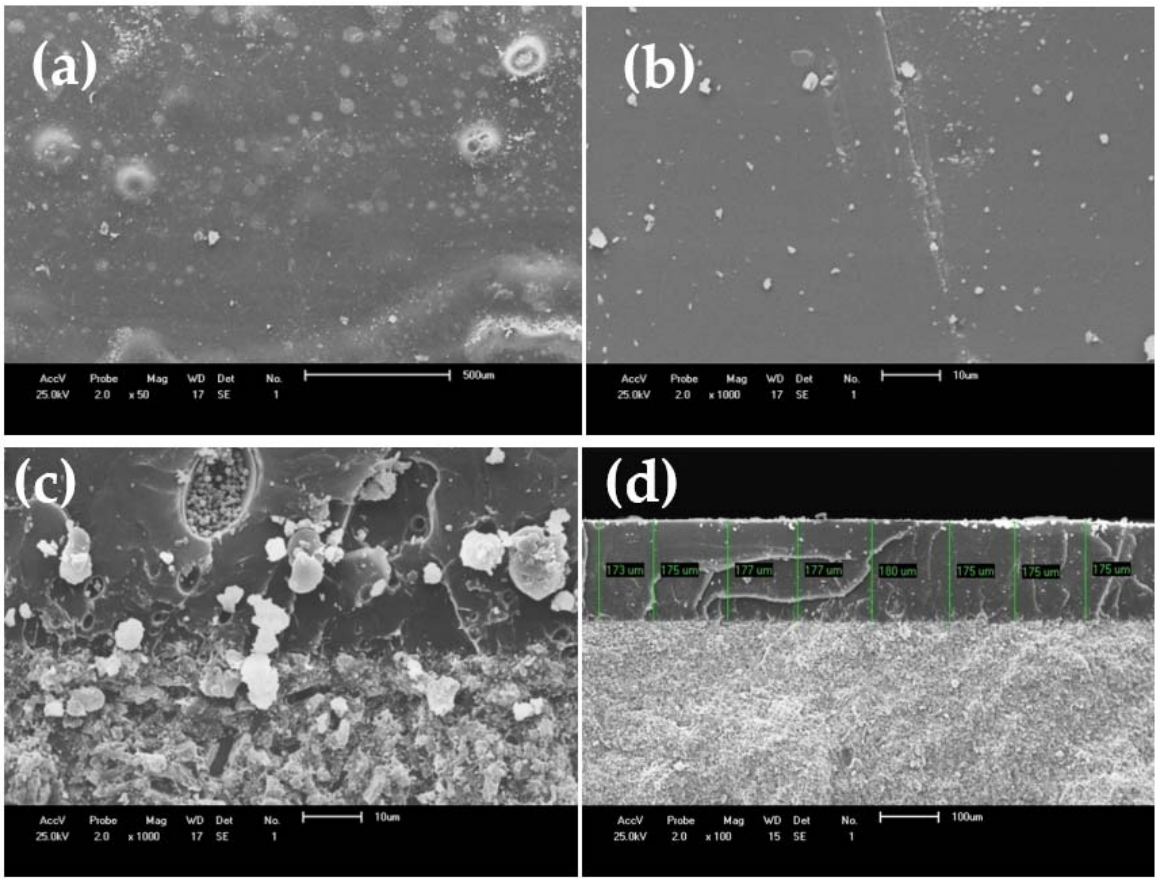

Figure 6. (**a**,**b**) SEM images from the surface, and (**c**) cross-section of Vitro-ceram infiltrated with PMMA for 6 h. (**d**) Sample cross-section image at lower magnification of ×100 and infiltration for 12 h.

The data for the water absorption, bulk density and porosity content of the sintered and infiltrated samples are summarized in Table 3. A reduction in the apparent porosity and, therefore, water absorption, ranging from 33–50%, is observed for all the samples after infiltration for 6 h and polymerization. A slight increase, considering the standard deviation, in the density is also observed. For a period of 12 h, under the same conditions described above, there was an even greater reduction in the apparent porosity and water absorption from 54 (Alglass) to 99% (Vitro-ceram). A small increase in the value of the density is also recorded, except for Vitro-ceram. The Vitro-ceram is less porous (before and after the infiltration) when compared to the other groups. This can be attributed to the fact that it has been well-pressed (i.e., it has higher density) due to its particle size distribution. According to German [17], the packaging of particles with bimodal size distribution results in higher densities than monomodal distribution packaging. The sample Vitro-ceram presented a range of particle size distributions with a greater number of smaller particles contributing to better packaging, a higher density and smaller pore size after sintering. This favored a more extensive filling of pores by monomer due to the greater capillary force.

Table 3. Infiltration time, density, porosity and water absorption of sintered and infiltrated alumina preforms.

Ceramic Samples	Infiltration Time (h)	Density (g/cm^3)	Porosity (%)	Water Absorption (%)
Alglass	0	2.6 ± 0.03	29.4 ± 0.6	9.9 ± 0.2
	6	2.8 ± 0.04	16.1 ± 3.9	5.4 ± 1.3
	12	2.8 ± 0.04	13.4 ± 2.6	4.5 ± 0.8
In-ceram	0	2.6 ± 0.08	33.1 ± 2.2	11.1 ± 1.0
	6	2.6 ± 0.23	21.0 ± 11.7	7.3 ± 4.3
	12	2.8 ± 0.06	13.6 ± 11.6	4.5 ± 3.8
Vitro-ceram	0	2.7 ± 0.01	28.1 ± 2.8	9.0 ± 0.09
	6	2.7 ± 0.34	18.8 ± 5.5	6.9 ± 1.6
	12	2.8 ± 0.07	0.2 ± 0.1	0.14 ± 0.07

Table 4 presents the statistical data of physical properties, in which the Tukey test for the comparison of the average values was performed at a significance level of 5%.

Table 4. Comparison of averages for water absorption, apparent porosity and bulk density of independent samples using Tukey test to the 5% level of statistical significance.

Ceramic Samples	Infiltration Time (h)	Average of Density (g/cm^3)	Average of Porosity (%)	Average of Water Absorption (%)
Alglass	0	2.6 ^{b}	29.4 ^{a}	9.9 ^{a}
	6	2.8 ^{a}	16.1 ^{b}	5.4 ^{b}
	12	2.8 ^{a}	13.4 ^{b}	4.5 ^{b}
		$p = 0.002$	$p < 0.001$	$p < 0.0001$
In-ceram	0	2.6 ^{a}	33.1 ^{a}	11.1 ^{a}
	6	2.6 ^{a}	21.0 ^{b}	7.3 ^{ab}
	12	2.8 ^{a}	13.6 ^{b}	4.5 ^{b}
		$p = 0.04$	$p < 0.001$	$p = 0.0023$
Vitro-ceram	0	2.8 ^{a}	28.1 ^{a}	9.0 ^{a}
	6	2.5 ^{a}	18.8 ^{b}	6.9 ^{b}
	12	2.6 ^{a}	0.2 ^{c}	0.1 ^{c}
		$p = 0.68$	$p < 0.001$	$p < 0.0001$

Note: Equal superscript letters mean statistically equal values and different letters mean statistically different values at a significance level of 5%.

According to the Tukey test at a 5% probability level (Table 4), the densities of the Alglass showed no statistically significant difference when infiltrated by periods of 6 and 12 h but showed differences concerning the control group (without infiltration). However, Vitro-ceram and In-ceram samples, when compared with the control group, do not show a statistically significant difference between 6 and 12 h time of infiltration.

With regard to porosity, there was no statistically significant difference for the different times of infiltrations for the Alglass and In-ceram samples. In contrast, the Vitro-ceram presented a statistically significant difference related to the infiltration time, where there was a significant reduction in porosity at the infiltration of 12 h than 6 h.

Considering water absorption, the Vitro-ceram showed a statistically significant difference with the infiltration times of 6 and 12 h and with the control group, showing a significant reduction in water absorption after infiltration. The control group corresponds to the sintered samples from each Al_2O_3 commercial powder without PMMA-infiltration. For the Alglass and In-ceram samples, there was no influence, statistically, in relation to the times of 6 and 12 h of infiltration, but a difference (reduction) was observed with regard to the control group.

This statistical analysis shows that changing the infiltration time has significantly influenced the properties of Vitro-ceram (porosity content and water absorption), whereas it does not affect Alglass and In-ceram.

The results for the mechanical tests are summarized in Table 5. The strength values observed for sintered samples are lower than those of infiltrated alumina because of the higher porosity [18]. After 6 and 12 h of infiltrations, all the samples showed a significant increase in strength ranging from 83% (for Alglass) to 218% (for Vitro-ceram). However, the values for Alglass and In-ceram are below those specified by ISO standard 6872 and close to PMMA (25 MPa), for example, at least 100 MPa for monolithic ceramic for a single-unit anterior or posterior prostheses adhesively cemented in the confection of infrastructure in fixed prostheses.

Table 5. Flexural strength and microhardness of alumina samples sintered at 1400 °C and infiltrated with PMMA.

Ceramic Samples	Infiltration Time (h)	Flexural Strength (MPa)	Microhardness (HV)
Alglass	0	9.0 ± 2.1	455.0 ± 36.6
	6	9.4 ± 5.1	468.8 ± 15.5
	12	16.5 ± 5.4	519.1 ± 39.5
In-ceram	0	41.0 ± 3.8	458.0 ± 28.2
	6	61.0 ± 7.7	704.0 ± 41.7
	12	75.9 ± 8.0	857.0 ± 55.1
Vitro-ceram	0	37.5 ± 17.6	439.0 ± 37.3
	6	78.8 ± 16.6	1030.7 ± 52.3
	12	119.3 ± 23.6	1055.1 ± 111.0
PMMA	–	25.0 ± 5.0	216.0 ± 41.7

According to Patel et al. [19], during monomer conversion to polymer (PMMA), an approximately 20% volume reduction occurs. In this case, this volume reduction in the infiltrated polymer in the alumina matrix creates voids due to the spatial separation between the two materials that diminish the composite ability to withstand higher applied loads [20]. However, the Vitro-ceram sample could be potentially selected for use in metal-free structures, for crowns and fixed partial prostheses. This can be supported by the good bending resistance and microhardness (119 MPa and HV 1055, respectively) [21].

Comparing the mechanical properties of polymer-infiltrated ceramics (PICs) with their contenders is beneficial, specifically when strength and hardness are evaluated. Albero et al. [21] have compared the three-point flexural strength values of some commercial PICs, whose composition was not clearly disclosed, and reported the strength of 180

and 164 MPa for Vita Enamic (Vita Zahnfabrik Co., Berlin, Germany.) and Lava Ultimate (3M Co., Sumaré, SP, Brazil), respectively. These materials have a strength lower than lithium disilicate glass-ceramic (Ivoclar Co., IPS e.max: ~270 MPa) and greater than feldspathic porcelain (Vita Co., Mark II: ~138 MPa) or leucite glass-ceramic (~160 MPa). Some other researchers have reported a strength of 100–150 MPa for PICs [22]. The hardness of PICs could also be compared with other materials. The lithium disilicate glass-ceramic shows a hardness of 5.83 GPa, followed by leucite-based glass-ceramic (4.60 GPa) and feldspathic porcelain (3.46 GPa). Most resin-reinforced PICs demonstrate values between 1.15–1.70 GPa, similar to dental tissues [22]. Therefore, the strength (~120 MPa) and hardness (~1.06 GPa) of Vitro-ceram are in the range of PICs suitable for restorative purposes.

Table 6 shows the flexural strength and microhardness measurements submitted to the Tukey test to the 5% statistical significance level. For the flexural test, the samples Vitro-ceram and In-ceram presented statistically different values, while the Alglass showed no differences. The microhardness of Vitro-ceram does not differ statistically when infiltrated for 6 and 12 h; however, the values for the In-ceram fluctuate statistically for different infiltration times and considering the control group. The Alglass sample showed a statistically significant difference when infiltrated for 6 or 12 h. Overall, these results confirmed that increasing the infiltration time, as expected, leads to a statistically significant increase in hardness and strength.

Table 6. Comparison of average flexural strength and microhardness of independent samples using Tukey test at 5% probability level.

Ceramic Samples	Infiltration Time (h)	Average of Flexural Strength (MPa)	Average of Microhardness (HV)
Alglass	0	9.0 ^{a}	455.7 ^{b}
	6	9.4 ^{a}	468.8 ^{b}
	12	16.5 ^{a}	519.1 ^{a}
		$p = 0.0737$	$p = 0.0003$
In-ceram	0	41.0 ^{c}	458.0 ^{c}
	6	61.0 ^{b}	704.9 ^{b}
	12	75.9 ^{a}	857.5 ^{a}
		$p < 0.0001$	$p < 0.0001$
Vitro-ceram	0	37.5 ^{c}	439.8 ^{b}
	6	78.8 ^{b}	1030.7 ^{a}
	12	119.3 ^{a}	1055.1 ^{a}
		$p < 0.0001$	$p < 0.0001$

Note: Equal superscript letters mean statistically equal values and different letters mean statistically different values at a significance level of 5%.

4. Conclusions

The infiltration of sintered Al_2O_3 (Vitro-ceram) by PMMA for 12 h under the pressure of 7 bar led to the development of a highly filled PMMA/ceramic composite for potential use as a dental prosthesis. The 12-hour infiltration for Vitro-ceram demonstrated a near-zero open porosity and optimum mechanical characteristics, passing the acceptance criteria of ISO 6872 and making it suitable for consideration as a metal-free structure for dental crowns and fixed partial prostheses until three anterior units. The near-zero surface porosity, well-matched density (2.60 ± 0.07 g/cm^3) and acceptable mechanical properties (strength and hardness equal to 119.3 ± 5.0 MPa and 1055.1 ± 111.0, respectively) were reported for this composite. However, further investigations on the biocompatibility (chemical degradation), aesthetic properties, machinability, hardness adjustment and fracture toughness are still necessary to clearly prove the suitability of this material for clinical applications. Additionally, the major limitation of the study was the low wetting of alumina by PMMA precursors, which made complete infiltration of the body impossible. Perhaps a surface treatment of alumina could be useful to change its surface tension in order to allow the wetting of the body by PMMA, thus yielding a more effective infiltration.

Author Contributions: Conceptualization, H.d.L.L., F.B. and R.R.M.; formal analysis, A.M.R. and M.M.; investigation, O.C.d.S.; data curation, O.C.d.S.; writing—original draft preparation, A.M.R. and M.M.; writing—review and editing, A.M.R., M.M., H.d.L.L., F.B. and R.R.M.; project administration, H.d.L.L., F.B. and R.R.M.; funding acquisition, H.d.L.L., F.B. and R.R.M. All authors have read and agreed to the published version of the manuscript.

Funding: The authors are grateful to the Brazilian research funding agency CNPq, grant nos. 308822/2018-8 and 420004/2018-1, for the financial support. The publishing costs were covered by F.B.

Institutional Review Board Statement: Not applicable.

Informed Consent Statement: Not applicable.

Data Availability Statement: Data are contained in the article.

Conflicts of Interest: The authors declare no conflict of interest.

References

1. Montazerian, M.; Zanotto, E.D. Bioactive and Inert Dental Glass-Ceramics. *J. Biomed. Mater. Res. A* **2017**, *105*, 619–639. [CrossRef] [PubMed]
2. Sakaguchi, R.L.; Powers, J.M. *Craig's Restorative Dental Materials*, 13th ed.; Elsevier, Mosby: Philadelphia, PA, USA, 2012; ISBN 978-0-323-08108-5.
3. Schmalz, G.; Watts, D.C.; Darvell, B.W. Dental Materials Science: Research, Testing and Standards. *Dent. Mater.* **2021**, *37*, 379–381. [CrossRef] [PubMed]
4. Ferracane, J.L. Current Trends in Dental Composites. *Crit. Rev. Oral Biol. Med.* **1995**, *6*, 302–318. [CrossRef] [PubMed]
5. Wang, Y.; Zhu, M.; Zhu, X.X. Functional Fillers for Dental Resin Composites. *Acta Biomater.* **2021**, *122*, 50–65. [CrossRef] [PubMed]
6. Lange, R.-T.; Pfeiffer, P. Clinical Evaluation of Ceramic Inlays Compared to Composite Restorations. *Oper. Dent.* **2009**, *34*, 263–272. [CrossRef] [PubMed]
7. Vanoorbeek, S.; Vandamme, K.; Lijnen, I.; Naert, I. Computer-Aided Designed/Computer-Assisted Manufactured Composite Resin versus Ceramic Single-Tooth Restorations: A 3-Year Clinical Study. *Int. J. Prosthodont.* **2010**, *23*, 223–230. [PubMed]
8. Gonzaga, C.C.; Yoshimura, H.N.; Cesar, P.F.; Miranda, W.G.J. Subcritical Crack Growth in Porcelains, Glass-Ceramics, and Glass-Infiltrated Alumina Composite for Dental Restorations. *J. Mater. Sci. Mater. Med.* **2009**, *20*, 1017–1024. [CrossRef] [PubMed]
9. Coldea, A.; Swain, M.V.; Thiel, N. Mechanical Properties of Polymer-Infiltrated-Ceramic-Network Materials. *Dent. Mater.* **2013**, *29*, 419–426. [CrossRef]
10. Zafar, M.S. Prosthodontic Applications of Polymethyl Methacrylate (PMMA): An Update. *Polymers* **2020**, *12*, 2299. [CrossRef]
11. Abdulkareem, M.M.; Hatim, N.A. Evaluation the Biological Effect of Adding Aluminum Oxide, Silver Nanoparticles into Microwave Treated PMMA Powder. *Int. J. Enhanc. Res. Sci. Technol. Eng.* **2015**, *4*, 172–178.
12. Chaijareenont, P.; Takahashi, H.; Nishiyama, N.; Arksornnukit, M. Effect of Different Amounts of 3-Methacryloxyprop yltrimethoxysilane on the Flexural Properties and Wear Resistance of Alumina Reinforced PMMA. *Dent. Mater. J.* **2012**, *31*, 623–628. [CrossRef] [PubMed]
13. Vojdani, M.; Bagheri, R.; Khaledi, A.A.R. Effects of Aluminum Oxide Addition on the Flexural Strength, Surface Hardness, and Roughness of Heat-Polymerized Acrylic Resin. *J. Dent. Sci.* **2012**, *7*, 238–244. [CrossRef]
14. Kul, E.; Aladağ, L.İ.; Yesildal, R. Evaluation of Thermal Conductivity and Flexural Strength Properties of Poly(Methyl Methacrylate) Denture Base Material Reinforced with Different Fillers. *J. Prosthet. Dent.* **2016**, *116*, 803–810. [CrossRef] [PubMed]
15. *ISO 6872:2015—Dentistry—Ceramic Materials*, 4th ed.; International Organization for Standardization: Geneva, Switzerland, 2015.
16. de Oliveira, I.R.; Studart, A.R.; Pileggi, R.G.; Pandolfelli, V.C. *Dispersão e Empacotamento de Partículas: Princípios e Aplicações em Processamento Cerâmico*; Fazendo Arte Editorial: Sao Paolo, Brazil, 2000.
17. Randall, M. *German Particle Packing Characteristics*; Metal Powder Industries Federation: Princeton, NJ, USA, 1999; ISBN 0918404835.
18. Coldea, A.; Swain, M.V.; Thiel, N. Hertzian Contact Response and Damage Tolerance of Dental Ceramics. *J. Mech. Behav. Biomed. Mater.* **2014**, *34*, 124–133. [CrossRef] [PubMed]
19. Patel, M.P.; Braden, M.; Davy, K.W.M. Polymerization Shrinkage of Methacrylate Esters. *Biomaterials* **1987**, *8*, 53–56. [CrossRef]
20. Franco Steier, V.; Koplin, C.; Kailer, A. Influence of Pressure-Assisted Polymerization on the Microstructure and Strength of Polymer-Infiltrated Ceramics. *J. Mater. Sci.* **2013**, *48*, 3239–3247. [CrossRef]
21. Albero, A.; Pascual, A.; Camps, I.; Grau-Benitez, M. Comparative Characterization of a Novel Cad-Cam Polymer-Infiltrated-Ceramic-Network. *J. Clin. Exp. Dent.* **2015**, e495–e500. [CrossRef] [PubMed]
22. Facenda, J.C.; Borba, M.; Corazza, P.H. A Literature Review on the New Polymer-Infiltrated Ceramic-Network Material (PICN). *J. Esthet. Restor. Dent.* **2018**, *30*, 281–286. [CrossRef] [PubMed]